Brain-Endocrine Interactions: A Microvascular Route in the Mediobasal Hypothalamus

Philippe Ciofi, Maurice Garret, Olivier Lapirot, Pierrette Lafon, Anne Loyens, Vincent Prévot, and Jon E. Levine

Institut National de la Santé et de la Recherche Médicale (INSERM) Unité 862 (P.C., O.L.), Neurocentre Magendie, and Université de Bordeaux (P.C., M.G., O.L.), F-33077 Bordeaux, France; Centre National de la Recherche Scientifique (M.G.), Unite Mixte de Recherche 5227, F-33077 Bordeaux, France; EA2972 (P.L.), Université de Bordeaux, F-33405 Talence, France; INSERM Unité 837 (A.L., V.P.), F-59045 Lille, France; Université de Lille 2 (A.L., V.P.), F-59045 Lille, France; and Department of Neurobiology and Physiology (J.E.L.), Northwestern University, Evanston, IL 60208

Blood-borne hormones acting in the mediobasal hypothalamus, like those controlling food intake, require relatively direct access to target chemosensory neurons of the arcuate nucleus (ARC). An anatomical substrate for this is a permeable microvasculature with fenestrated endothelial cells in the ARC, a system that has awaited comprehensive documentation. Here, the immunofluorescent detection of endothelial fenestral diaphragms in the rat ARC allowed us to quantitate permeable microvessels throughout its rostrocaudal extent. We have determined that permeable microvessels are part of the subependymal plexus irrigating exclusively the ventromedial (vm) ARC from the subadjacent neuroendocrine median eminence. Unexpectedly, permeable microvessels were concentrated proximal to the pituitary stalk. This marked topography strongly supports the functional importance of retrograde blood flow from the pituitary to the vmARC, therefore making a functional relationship between peripheral long-loop, pituitary short-loop, and neuroendocrine ultra-short loop feedback, altogether converging for integration in the vmARC (formerly known as the hypophysiotrophic area), thereby so pivotal as a multicompetent brain endocrinostat. **(*Endocrinology* 150: 5509–5519, 2009)**

For many decades, endocrinologists have suspected that circulating polypeptide hormones can rapidly enter the hypothalamus through a privileged route that bypasses the protection of the blood-brain barrier (BBB). This topic has been particularly revitalized in the recent years when obesity research has focused on the integrative functions of the arcuate nucleus (ARC), a primary target of convergent feedback by peripheral hormones like ghrelin, insulin, or leptin (see Ref. 1–8). The mechanism by which these hormones enter the ARC, however, has remained unclear. Potentially, three avenues may be used to convey hormones from the peripheral circulation to the sensor neurons of the ventromedial (vm) ARC (9–17). The first of these is the transcytosis from plasma to brain parenchyma through endothelial and glial elements of the BBB. A second possibility is via the paravascular route, whereby hormones would exit the permeable neuroendocrine capillaries of the neighboring median eminence (ME) and dissipate through the cerebrospinal fluid, bathing the coalescent perivascular spaces of the ARC/ME unit. A third possible route, long suspected to be a feature of the subependymal plexus (SEP), is a specific vascular channel irrigating the vmARC for fast transport. The capillaries of the SEP course in the walls of the infundibular recess of the third ventricle. They are the sole arterial afferents to the vmARC and are anastomosed with the intrainfundibular capillary loops of the ME. The SEP is thus a dorsal derivation of the hypothalamo-hypophysial vasculature (see Ref. 10). As such, it is well placed to drain arterial blood from the ME up to the vmARC, where it is expected to display highly permeable, fenestrated endothelial cells, as seen in the circumven-

ISSN Print 0013-7227 ISSN Online 1945-7170
Printed in U.S.A.

doi: 10.1210/en.2009-0584 Received May 20, 2009. Accepted August 25, 2009.
First Published Online October 16, 2009

Abbreviations: ARC, Arcuate nucleus; BBB, blood-brain barrier; CVO, circumventricular organ; HuC/D, human neuron-specific-mRNA binding proteins HuC/HuD; ME, median eminence; NKB, neurokinin B; NPY, neuropeptide Y; PB, phosphate buffer; PV1, plasmalemmal vesicle-associated protein 1; PV1-ir, PV-1 immunoreactive/immunoreactivity; RECA1, rat endothelial cell antigen 1; SEP, subependymal plexus; VB, veronal buffer; vmARC, ventromedial ARC; VPG, visceromotor pattern generator.

tricular organs (CVOs) forming the brain-periphery interface outside the BBB (18).

However, morphological evidence for permeable capillaries in the vmARC is surprisingly scant in the face of growing efforts by the endocrine community to understand feedback control of hypothalamic physiological regulatory mechanisms, such as those that govern energy homeostasis. Only two ultrastructural studies, including one by us, identified fenestrated endothelial cells in the vmARC (14, 16). In our own attempt (16), we encountered the two main difficulties inherent to the vmARC/ME region. First, it is a notoriously fragile tissue, and excellent ultrastructural preservation is infrequently obtained. Second, the local vascular network including the SEP is highly complex, which makes it an overwhelming task to derive topographic information from electron microscopic observation. Both of these difficulties have resulted in limited functional interpretation of histological data from a region where structure-function relationship is relatively well understood. Thus, the question remains, to what extent are afferent microvessels to the ARC permeable, and precisely which part of the nucleus do they irrigate?

To bring a clear answer to this, it would be satisfying to sort out phenotypically permeable vessels among the local arborizing vasculature. Highly permeable endothelial cells are perforated by pores, also known as fenestrations. In CVOs, like in endocrine glands or kidney tubules for instance, these fenestrations are occupied by a meshwork of radial fibrils, known as a diaphragm, from its ultrastructural aspect of opercula, or thin electron-dense material, across the fenestral pore (19, 20). Recently, a component of these fenestral diaphragms was isolated and named plasmalemmal vesicle-associated protein 1 (PV1) (21). It is thought that coiled PV1 homodimers constitute individual radial fibrils in fenestrations (20). Thus, to visualize highly permeable microvessels, we prepared an antiserum to PV1 that allowed us to localize and quantify fenestrated capillaries by light-microscopic immunocytochemistry in a large series of thick sections regularly spaced throughout the ARC/ME complex. Our study was conducted in rats and compared males with regularly cycling females, because the SEP receive a sexually dimorphic innervation evoking the link between metabolism and reproduction (16, 22–25). Furthermore, as a first attempt to evaluate the eventuality of a regulation of the diaphragm-forming PV1 under strictly physiological conditions, we also studied females taken at different times over the day of proestrus. In the late afternoon of that day, there occurs the most predictable, easily identifiable, and large-scaled burst of endocrine activity that sets into coordinated motion several neuroendocrine axes and their associated peripheral responses. This was therefore of immediate interest in the context of a morphofunctional study of brain-endocrine interactions.

We show here that fenestrated microvessels in both sexes are indeed part of the SEP; they course in the rostrocaudal extent of the vmARC and are bordered by those neurons defined as appetite-regulators by obesity research. These findings reveal a route by which peripheral hormones can reach arcuate sensor neurons for delivering fast/acute feedback information. As a corollary, peripheral hormones must deliver another type of feedback information, slow/chronic, by their saturable transport across the BBB. Thus, the present study delineates one possible mechanism for rapid hormonal feedback to the mediobasal hypothalamus (presented partly in abstract form in Ref. 26).

Materials and Methods

Animals

Wistar rats bred in our facilities (lights on 0730–1930 h) with food and water *ad libitum* were studied when 4 months old. We also used tissue sections (stored frozen from a previous study; see Ref. 27) from males and females killed 48 h after colchicine treatment (for each, n = 2). All efforts were made to minimize the number of animals used and any distress caused by the procedures. They were killed (after an overdose of 20% chloral hydrate) in accordance with the European Communities Council Directive of November 24, 1986 (86/609/EEC).

Experiments

Two experiments, taking into account the sexually dimorphic innervation of the SEP (16, 27), were carried out independently and therefore analyzed separately. The first experiment searched for a sex-dimorphism and/or a cyclic variation in the distribution of PV1 immunoreactivity (PV1-ir) in vmARC and compared males (n = 12, killed from 1000–1400 h) and females killed either on the day of diestrus 1 (at 1000 h, D1, n = 10) or proestrus (at 1000 h, P10, n = 7; at 2000 h, P20, n = 9). The second experiment searched for a transient variation of PV1-ir in vmARC during the preovulatory surge of LH, *i.e.* during a sustained, generalized secretory activity. For this, females were killed every 2 h on the day of proestrus (0800–2200 h; n = 4–6/time point).

Preparation of rabbit polyclonal antisera to PV1 and controls

Two rabbits were immunized with a synthetic PV1 C-terminal peptide (KGPPLVNPAVPPSG) as in Ref. 28, and one batch of immuneserum (coded IS-104) was affinity-purified on HiTrap NHS-activated HP affinity column (Amersham Biosciences, Little Chalfont, UK). Purified IS-104 was used, diluted 1:200 and 1:2000 for light and electron microscopy, respectively. Specificity controls included: 1) immunoblotting characterization of the PV1-ir material in protein extracts from several organs including the vmARC/ME; 2) isolation, cloning, and sequencing of hypothalamic PV1 mRNA; 3) localization of PV1 mRNA in brain by *in situ* hybridization; 4) immunohistochemical localization of PV1-ir in the microvasculature of selected organs with (endocrine glands and lung) or without (liver and kidney glomerulus) diaphragms; and 5) electron microscopic evidence of binding of

purified antibodies at fenestral diaphragms in the hypothalamo-hypophysial vasculature. For a description of the procedures, see Refs. 16, 29, and 30. See supplemental data, published on The Endocrine Society's Journals Online web site at http://endo.endojournals.org for details.

Additional antisera

We also used a guinea pig anti-GnRH (1:2000; code IS-8; see Ref. 31), a mouse monoclonal to the panendothelial cell-specific antigen, rat endothelial cell antigen 1 (RECA1), for labeling blood vessels (1:250; catalog no. MCA970R; AbD Serotec, Cergy Saint-Christophe, France) (27), a mouse monoclonal to the neuron-specific, mRNA binding, human proteins HuC/HuD (HuC/D; 1:750; Molecular Probes catalog no. A21271; Invitrogen SARL, Cergy-Pontoise, France), a guinea pig anti-neurokinin B (NKB) to visualize sexually dimorphic perivascular axons (1:2000; code IS-3/61) (32), a sheep anti-α-MSH (1:2000; Chemicon catalog no. AB5087; Millipore S.A.S., Guyancourt, France), and a guinea pig antihuman neuropeptide Y (NPY; 1:3000; code IS-CNPY) prepared by coupling the full-length synthetic peptide (NeoMPS S.A., Strasbourg, France) to human serum albumin with glutaraldehyde; specificity was controlled by preabsorption and dual labeling with a well-characterized rabbit anti-NPY (see Ref. 16 and Ciofi, P., unpublished data). Secondary antisera were donkey IgGs linked to cyanine dye 2 (Cy2), tetramethyl rhodamine isothiocyanate (TRITC), or aminomethyl-coumarin-acetate (AMCA; 1:300; Jackson ImmunoResearch Laboratories, West Grove, PA).

Immunocytochemical procedure

For light microscopy, tissues were perfusion-fixed with 4% paraformaldehyde in a 0.2 M borate buffer (pH 9.5; semiquantitative analyses), or 2% paraformaldahyde/0.2% picric acid in 0.1 M phosphate buffer (PB, pH 7.4) (27). Serial cryostat sections were collected in a 0.1 M veronal buffer (VB, pH 7.4; 50 μm thick, semiquantitative analyses) or onto gelatinized slides (12 μm thick). Antisera were diluted in VB, containing 0.25% Triton X-100 (VB-TX), and applied at room temperature either overnight (primaries) or for 2 h (secondaries). Observation was on Epifluorescence (Zeiss Axiophot 1 equipped with a Leica DFC300X video camera) and confocal (Leica DMR TCS SP2 AOBS) microscopes (Carl Zeiss S.A.S., Le Pecq, France; Leica Microsystems France, Rueil-Malmaison, France). For electron microscopy, a preembedding immunogold procedure was followed. Briefly, brains were perfusion-fixed with 4% paraformaldehyde/1% glutaraldehyde in PB, and dissected ARC/ME blocks were cryostat-cut into 45-μm-thick slices that were incubated at 4 C, first in purified IS-104 for 72 h, then in colloidal gold (18nm)-labeled goat antirabbit IgGs (overnight, 1:20 in PB; Jackson Immunology). Slices embedded in Araldite and ultrathin sections were prepared for observation in a Zeiss TEM 902 (Leo, Reuil-Malmaison, France) equipped with a Gatan Orius SC1000 CCD camera (Gatan France, Grandchamp, France). See supplemental data for details.

Semiquantitative estimates of vascular permeability in the vmARC

One-in-three series of frontal sections were triple-labeled for PV1 (using Cy2, shows endothelial fenestrations), RECA1 (using TRITC, shows all endothelial cells) and GnRH (using AMCA, helps for arrangement). Digital images (×10 objective) of PV1 and RECA1 labeling were arranged rostrocaudally, matched across animals by anatomical plane, and analyzed (MetaMorph 6.2; Universal Imaging Corp., West Chester, PA). The vmARC was sampled bilaterally (excluding all capillaries of the ME proper as in Ref. 27) to quantify two parameters of vascular permeability: 1) the number of (RECA1-immunoreactive) capillary profiles with PV1-ir (one same profile with several PV1-ir spots was counted as one), and 2) the number of PV1-ir pixels. See supplemental data for details.

RIA for serum LH

To determine the time of the surge of LH in female rats killed in proestrus, right atrial blood was collected before perfusion and serum was stored at −20 C until assay. Serum LH levels were determined by using RIA reagents obtained from the National Institute of Diabetes and Digestive and Kidney Diseases (National Institutes of Health, Bethesda, MD), including LH reference RP-3 and S-11 antibody. The assay had a lower limit of detection of 0.2 ng/ml, and the intraassay coefficient of variance was 14.7%.

Statistical analysis

To search whether the two parameters of vascular permeability exhibited topography, sex-dimorphism, or cyclic variation in the ARC, sections (>1500) were all quantified in duplicates, and individual values were averaged to get mean section plane values that were compared by a two-way ANOVA for repeated measures followed if significant by a *post hoc* Tukey's multiple comparison test. Section planes 17–22 exhibited no PV1-ir in vmARC and were excluded from the statistical analysis. Detailed results of ANOVA are given in supplemental Table 1. Serum LH values were compared by a one-way ANOVA followed by a Tukey's multiple comparison test. All values are shown as mean ± SEM.

For details of the materials and methods used, see supplemental data.

Results

PV1 is expressed in the endothelium of CVOs and pituitary

Immunoblotting

In protein extracts from various tissues, and in reducing conditions, our purified anti-PV1 IgGs revealed one major (in some cases diffuse) band of material with an apparent molecular weight that was organ-specific (Fig. 1A). This, together with the presence of several minor bands, suggested various glycosylated forms. PV1 is probably nonglycosylated in the vmARC/ME because the approximately 60-kDa PV1-ir material in lung extracts also migrated at about 50 kDa (predicted mass of PV1 primary sequence) after deglycosylation treatment.

Extraction and sequencing of hypothalamic PV1 mRNA

Reinforcing deglycosylation experiments, PV1 mRNA extracted from vmARC/ME and amplified by RT-PCR exhibited a nucleotide sequence in the open-reading frame strictly matching the sequence found by Stan *et al.* (28), with no evidence for splicing or editing (not shown).

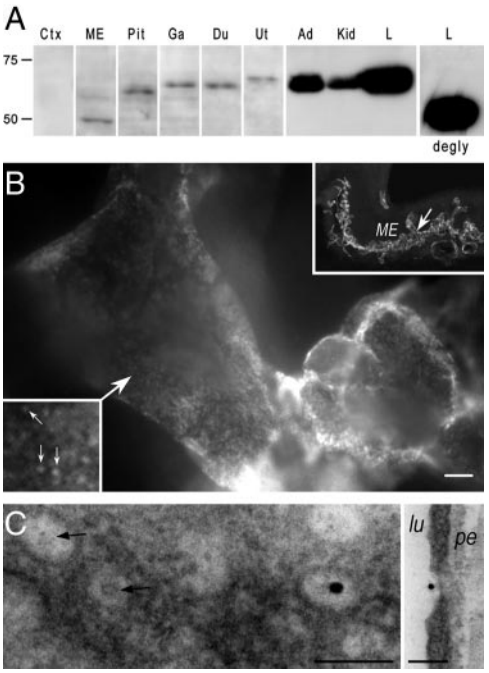

FIG. 1. Specificity controls of the affinity-purified anti-PV1 rabbit IgGs. A, Immunoblotting of total membrane proteins (all lanes from one same gel) from cerebral cortex (Ctx, 100 mg), vmARC/ME (ME, 6 mg), whole pituitary (Pit, 20 mg), gastric antrum (Ga, 15 mg), duodenum (Du, 30 mg), uterus (Ut, 3 mg), adrenal gland (Ad, 20 mg), kidney (Kid, 20 mg), and lung (L, each 20 mg). Molecular masses (kDa) of markers (Bio-Rad, Marnets-la-Coquette, France) are on the left. Note the position of the ME band and that deglycosylation pretreatment (degly) reveals an apparent mass of 50 kDa consistent with the 50.04 kDa deduced from the open reading frame of the mRNA sequence. B, PV1 labeling over endothelial cells in the external zone of the ME (*arrow in upper inset*). The *lower inset* shows disk-shaped labeled structures (*thin arrows*; digitally enlarged from main view taken with a ×100 oil-immersion objective). *Bar*, 1 μm. C, Electron micrographs of two ultrathin sections (*left*, tangential; *right*, transverse) through external ME capillaries exhibiting immunogold (18 nm) labeling for PV1 at the central knob of fenestral diaphragms (*arrows*, discernible knobs without overlying immunogold). lu, Capillary lumen; pe, perivascular space. *Bars*, 100 nm.

Detection of PV1 mRNA in brain by in situ hybridization

Hybridization signal (Fig. 2) was detected exclusively over highly permeable regions of the brain: organum vasculosum laminae terminalis, subfornical organ, choroid plexi, vmARC/ME, pineal gland, and area postrema. Over the BBB-protected neuropil, over the subcommissural organ, or after use of a sense probe, only low background signal was detected.

Light microscopic immunocytochemistry

Peripheral tissues. Endothelial cell types devoid of PV1 (20, 21) were PV1-negative (in striated muscle, kidney glomeruli, and liver sinusoids), whereas bright labeling was seen elsewhere (in kidney tubules, adrenal, lung, pancreas, *etc.*). Confocal microscopy showed that all PV1-ir structures were also RECA1-ir (not shown).

Brain and pituitary. Matching *in situ* hybridization data, PV1-ir endothelial cells were only seen in the organum vasculosum laminae terminalis, the subfornical organ, the choroid plexi, the vmARC/ME, the pineal gland, and the area postrema (Fig. 3). In the pituitary, virtually all blood vessels were PV1-ir (supplemental Fig. 1). No PV1-ir was seen in the subcommissural organ or BBB-protected areas. By confocal microscopy, all PV1-ir structures were also RECA1-ir (Fig. 3). By conventional epifluorescence with a ×100 oil-immersion objective, PV1-labeling could be resolved as individual fluorescent puncti (Fig. 1B).

Electron microscopic immunocytochemistry

Examination of the primary capillary plexus in the external zone of the ME at a high magnification (×85,000) revealed particle decoration at the central knob of fenestral diaphragms expected to host the C-terminal epitope of PV1 (Fig. 1C).

PV1-ir capillaries in the vmARC are bordered by appetite-regulating neurons and sexually dimorphic axons

The whole hypothalamo-hypophysial vascular unit was PV1-ir (Fig. 4A and supplemental Fig. 2): long portal vessels, primary superficial (hexagonal) plexus of the external zone of the ME, intrainfundibular capillary loops, and the SEP both in the ME and especially in the vmARC. In the vmARC, PV1-ir SEP capillaries were bordered by compact groups of cell bodies labeled for the neuronal marker HuC/D (Fig. 4A). Confocal microscopy and triple-labeling in colchicine-treated animals revealed that some of these perikarya are anorexigenic α-MSH-ir and orexigenic NPY-ir neurons (Fig. 4B; compare with ultrastructure in Ref. 16). Confocal microscopy and triple-labeling in normal animals further revealed that the sexually dimorphic NKB-ir innervation selectively concentrates around the PV1-ir microvessels (Fig. 4C). In the vmARC/ME, PV1-negative/RECA1-ir profiles were also present (pre- and postcapillary vessels).

PV1-ir capillaries concentrate proximal to the pituitary stalk in the vmARC

Followed in adjacent thick sections, the PV1-ir SEP capillaries of the vmARC anastomosed with the intrainfundibular capillary loops of the ME (Fig. 5A). In exceptional instances, this anatomical link could be fully observed within the thickness of a single section (supplemental Fig. 3). PV1-ir microvessels were infrequently observed rostrally in vmARC and were never observed caudal to plane 16. Section planes 11–14 (~−3.3–−3.9 mm from bregma according to Ref. 33), *i.e.* the ventral-most walls of the infundibular recess of the third ventricle, were enriched in PV1-ir capillary profiles and PV1-ir pixels (Fig. 5B). This topographical distribution of PV1-labeling clearly came

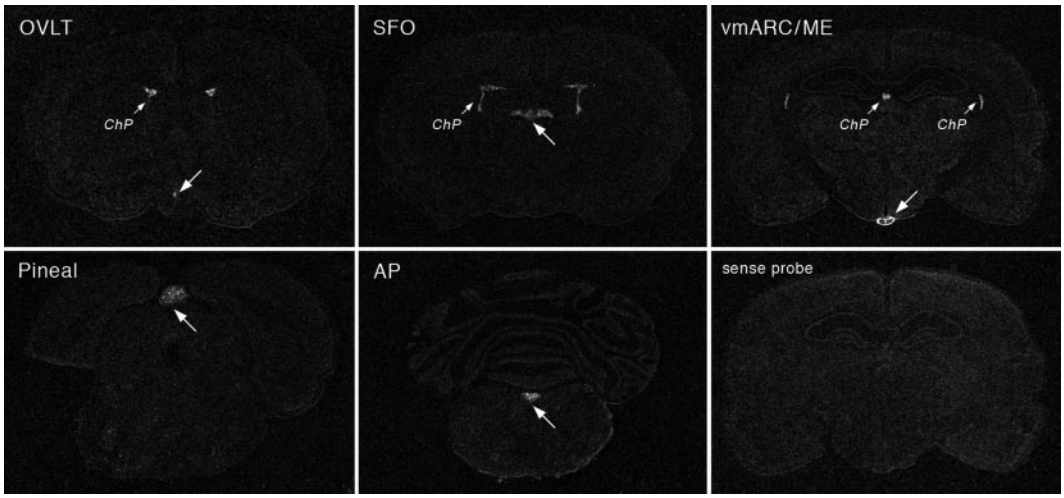

FIG. 2. Overview of PV1 mRNA expression in the brain of a male rat. PV1 mRNA expression is restricted to the CVOs and the pineal gland (*thick arrows*). Autoradiographic films after exposure to frontal sections hybridized with antisense or sense cRNA probes. Choroid plexi (ChP) are indicated by *thin arrows*. AP, area postrema; OVLT, organum vasculosum laminae terminalis; SFO, subfornical organ.

from the statistical analysis. Indeed, when the distribution of PV1-ir was compared using ANOVA between males and females taken at diestrus 1000 h (D10) and proestrus 1000 h and 2000 h (P10 and P20, respectively) only topography bore significant influence, both for the distribution of PV1-ir profiles ($P < .0001$) and PV1-ir pixels ($P < .0001$). No effect of sex or cycle day/hour could be detected (see Fig. 6A and supplemental Table 1).

PV1-ir varies under physiological circumstances

The occurrence of the surge of LH was efficiently captured in proestrous females because mean serum LH values were significantly elevated at 1800 h, 2000 h, and 2200 h (11.22 ± 0.45, 29.67 ± 1.99, and 16.00 ± 1.72 ng/ml, respectively), compared with low morning and afternoon values ($P < 2.50$ ng/ml and $P < .0001$, respectively; see supplemental Table 2). When the distribution of PV1-labeling was compared between the eight time groups taken individually, as above, between P10 and P20 females, the sole determinant was again topography (profiles, $P<.0001$; pixels, $P<.0001$; see Fig. 6B1 and supplemental Table 1). However, when animals were grouped according to their low (0800–1600 h; n = 23) or high (1800–2200 h; n = 14) LH values and compared altogether, topography (profiles, $P < .0001$; pixels, $P < .0001$) as well as an interaction between topography and LH values bore significance (profiles, $P < .0157$; pixels, $P < .0001$) (Fig. 6B2). *Post hoc* Tukey's multiple comparison test revealed that during the preovulatory surge of LH there was significantly more PV1-ir signal in vmARC at plane 11 (1.59 ± 0.24 *vs.* 3.17 ± 0.29 PV1-ir profiles/section; low *vs.* high LH, respectively; $P < .01$) and at plane 12 (2060.36 ± 311.02 *vs.* 3121.75 ± 236.66 PV1-ir pixels/section; low *vs.* high LH, respectively; $P < .01$).

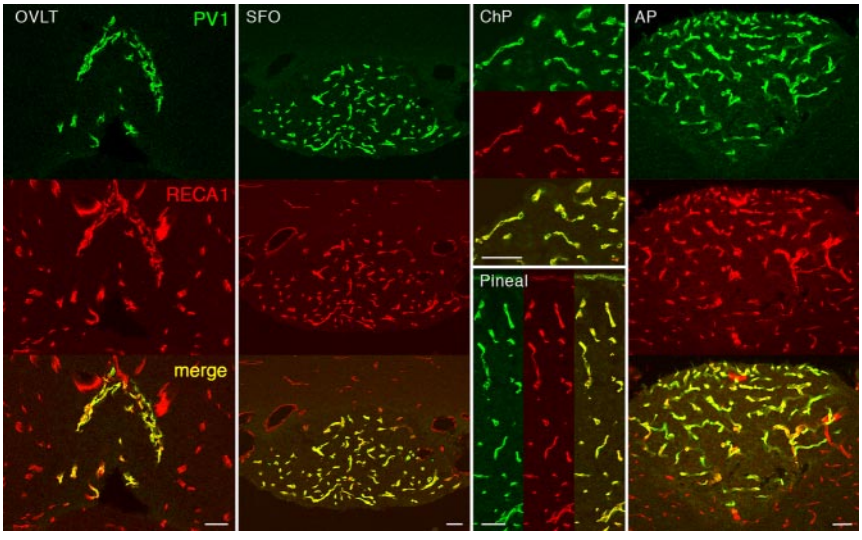

FIG. 3. Overview of PV1-ir in brain of a male rat. PV1-ir decorates a majority of blood vessels in the CVOs and the pineal. Frontal sections double-labeled for PV1 (*green*) and the panendothelial cell marker RECA1 (*red*). Single optical sections (1.52 μm thick) from confocal microscopy. Note that blood vessels outside CVOs are PV1-negative and that all PV1-ir structures are also RECA1-positive. See Fig. 2 for legends. *Bars*, 50 μm.

Discussion

Although the observation of an abundance of permeable microvessels in the ARC is critical to the development of our understanding of the mechanisms

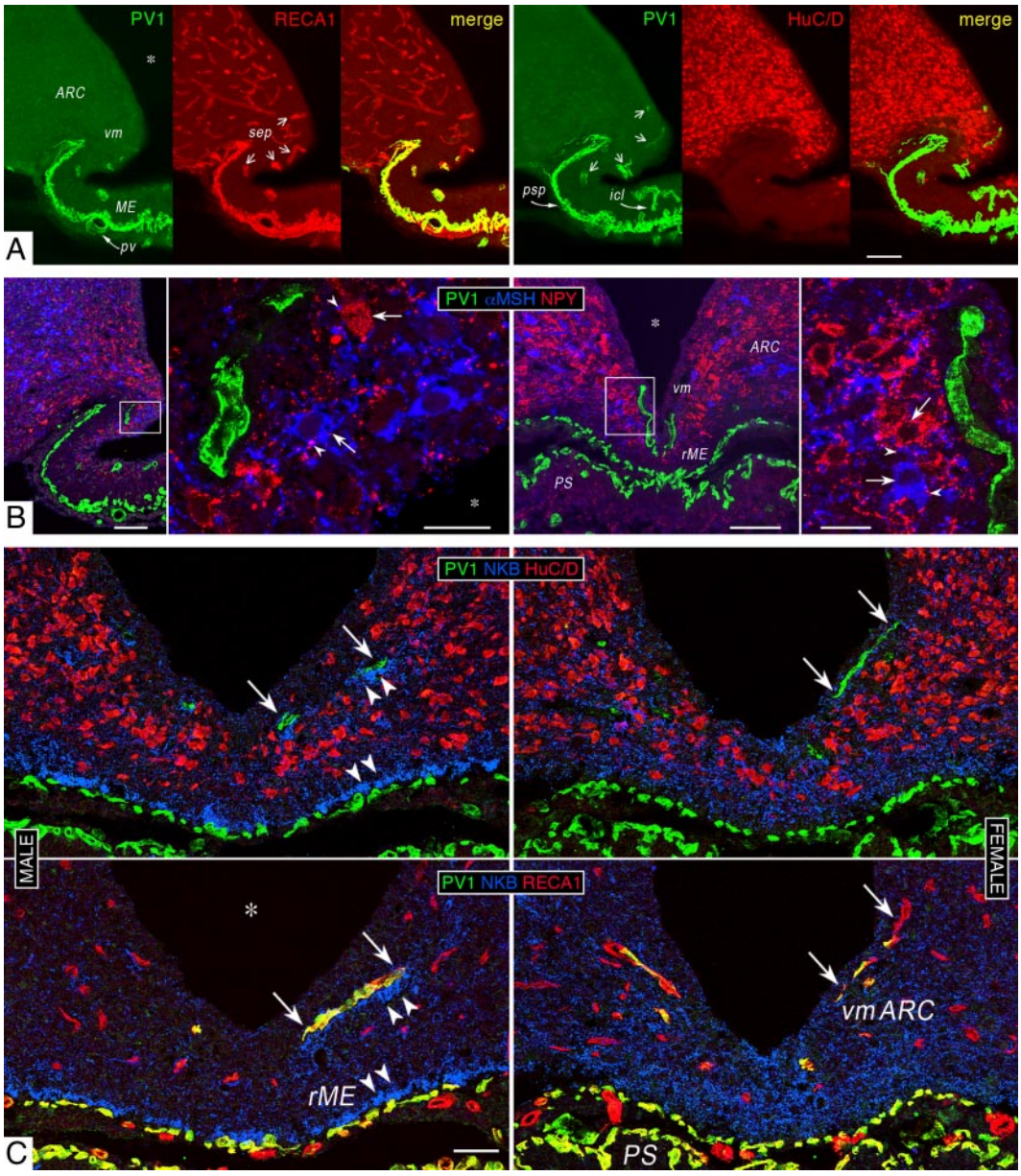

FIG. 4. Permeable microvessels of the vmARC are bordered by chemosensory neurons and sexually dimorphic axons. A, PV1-labeling decorates all subsets of the vasculature of the vmARC/ME. Two adjacent frontal sections (50 μm thick; ~−3.4 mm from bregma) double-labeled for PV1 (*green*) and either (*red*) the panendothelial cell marker RECA1 or the neuronal marker HuC/D (in merged images, PV1-signal is contrasted for clarity). In the vmARC (vm) numerous HuC/D-ir perikarya are close to PV1-ir subependymal capillaries (*right*, *short arrows*). icl, Intrainfundibular capillary loop; psp, primary superficial plexus; pv, long portal vessel; sep, subependymal plexus. *, Third ventricle. *Bar*, 100 μm. Normal male rat. B, Arcuate NPY/orexigenic and αMSH/anorexigenic sensor neurons lie in the vicinity of PV1-ir capillaries. Two frontal cuts at mid- (*left*) and retroinfundibular (*right*; ~−3.8 mm from bregma) levels after triple-labeling (PV1, *green*; αMSH, *blue*; NPY, *red*) with high magnification views of *boxed areas*. *Arrows* point to peptidergic perikarya and *arrowheads* to putative reciprocal contacts. Optical sections from confocal microscopy (high powers are 0.38 μm thick). PS, Pituitary stalk; rME, retroinfundibular ME. *Bars*, 100 μm (low-power views) and 10 μm (high-power views). Two colchicine-treated females. C, Permeable PV1-ir (*green*, *arrows*) microvessels have similar distribution in the vmARC and rME in both sexes but are bordered by palisades of NKB-ir axons (*blue*,*arrowheads*; purposely lightened for contrast) in males only. *Red* labeling is either for HuC/D or RECA1, as indicated. Single 1.52-μm-thick optical cuts of triple-labeled, adjacent cryostat sections (~−3.8 mm from bregma) from normal rats. *Bar*, 50 μm.

of control of energy homeostasis (and may be discussed solely along these lines), it may also more generally improve our knowledge of the humoral dialogue between the brain and peripheral tissues. The discovery of the adipocyte hormone leptin together with the obesity epidemic has rapidly made this peripheral hormone perhaps one of the best-studied circulating polypeptides for its effects at the hypothalamus. Yet, much remains to be clarified of the mechanisms of action of a prototypical hypothalamotrophic hormone, as discussed below.

In agreement with previous data from peripheral tissues (20, 21), the affinity-purified antibodies recognized PV1

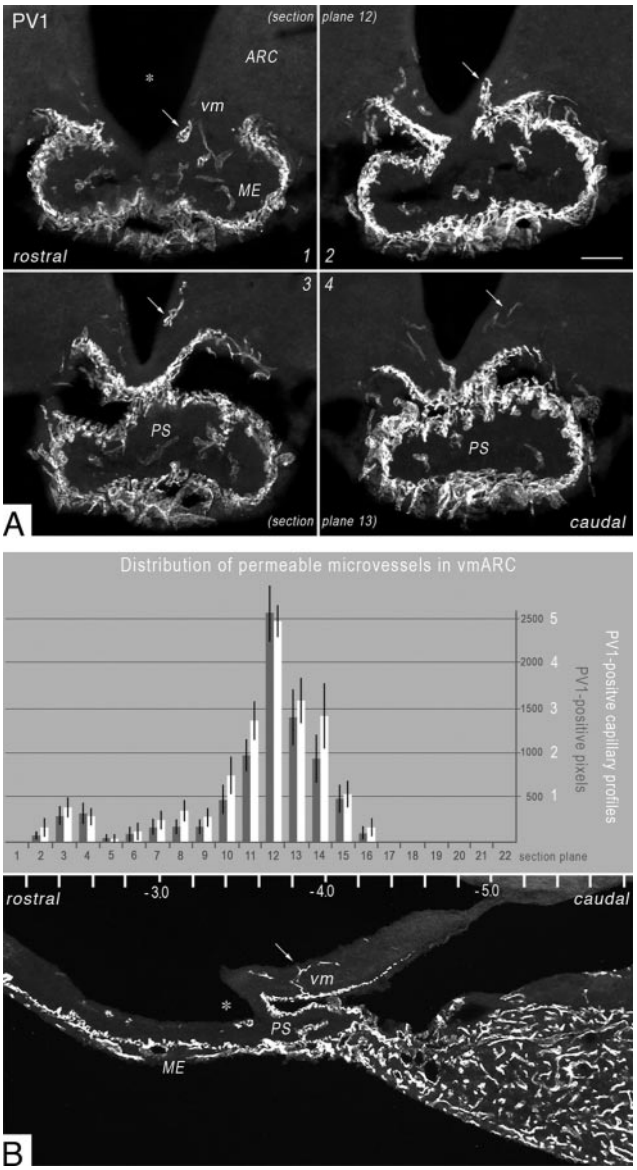

FIG. 5. Topographic distribution of PV1-ir capillaries in the vmARC. A, The highly permeable portion of the vmARC proximal to the pituitary stalk (PS). Labeling for PV1 in consecutive frontal sections (50 μm thick) revealing how sinusoidal capillaries branch up from the primary superficial plexus (*arrow* in 2) to give off ramifications of the subependymal plexus (*other arrows*) in the vmARC (vm). Labeling is variable among capillaries. Female rat at 1800 h on proestrus. *, Infundibular recess of the third ventricle. *Bar*, 100 μm. B (*Upper panel*), Topographical analysis in male rats (n = 12) of the number (mean ± SEM) of capillary profiles (RECA1-ir) with PV1-labeling (*white bars*) and numbers of PV1-ir pixels (*gray bars*) after bilateral sampling of the vmARC in coronal 50-μm-thick sections regularly spaced by 150 μm. Permeable microvessels were more frequently observed proximal to the pituitary stalk (planes 11–14). Most section planes significantly differed from one another by ANOVA, which is not indicated for purpose of clarity. B (*Bottom panel*), Cryostat-cut parasagittal section of a male rat hypothalamus after labeling for PV1 showing a permeable sinusoid (*arrow*) entering the retroinfundibular vmARC (vm) about −3.9 mm from bregma at section plane 14.

from different organs, and they bound ultrastructurally to the central knob of fenestral diaphragms in the brain. The presence of PV1 mRNA and protein in all CVOs and choroid plexi, as well as in the pineal and pituitary glands, conforms to the previous descriptions of the presence of microvessels with diaphragmed fenestrations in these tissues known for their exchange properties (18). Previous studies reporting the expression of PV1 in brain tissue have examined malignant tumors that are also known to harbor a highly permeable neovasculature exhibiting fenestral diaphragms (34, 35). The presence of PV1 thus indicates a high permeability for brain microvessels, either physiological or pathological, and physiological expression of PV1 is in areas where penetration of blood-borne proteins is facilitated (12). Immunoblotting suggested that PV1 is nonglycosylated in the vmARC/ME, which is a novel observation. This absence of sugars may confer a greater permeability to endothelial fenestrations (36) expected here to sustain intense bidirectional transport of polypeptides. It would be interesting to characterize the level of PV1 glycosylation in the other CVOs to test whether it is a unique feature of the vmARC/ME microvasculature.

Little is known about the mechanisms that may regulate expression of the diaphragm-forming PV1 (20). We have observed a significant increase in PV1 labeling late on proestrus, suggesting for the first time that the expression of the protein may be regulated in response or in anticipation of alterations in peripheral hormone actions in the vmARC. Increased labeling for PV1 suggests an increased number of fenestrations. This increased number of fenestrations would in turn suggest an increased permeability of vmARC vasculature during the surge of LH and therefore also suggest adaptation to feedback of pituitary/peripheral origin (see below). Adaptation of the permeability of the mediobasal hypothalamus to feedback regulators may thus constitute an important and previously unsuspected mechanism that gates hypothalamic neurons to feedback. The proximal determinants of any such alterations remain to be identified.

This proestrous variation in PV1 labeling was detectable in only a portion of the ARC, and may thus appear more limited than expected if compared with the large burst of endocrine activity occurring at that time. Our procedures and current assumptions probably misestimate the amplitude and/or physiological importance of such a variation in labeling for PV1. It is unlikely that the sampling procedure failed to include important section planes, which may have compromised full evaluation of the variation. We intentionally examined a large number of animals, and several large series of closely neighboring sections were collected. This certainly minimized potential sampling artifacts and allowed statistical identification of a proestrous variation. Additionally, the selective permeability of fenestrated endothelial cells may be modulated

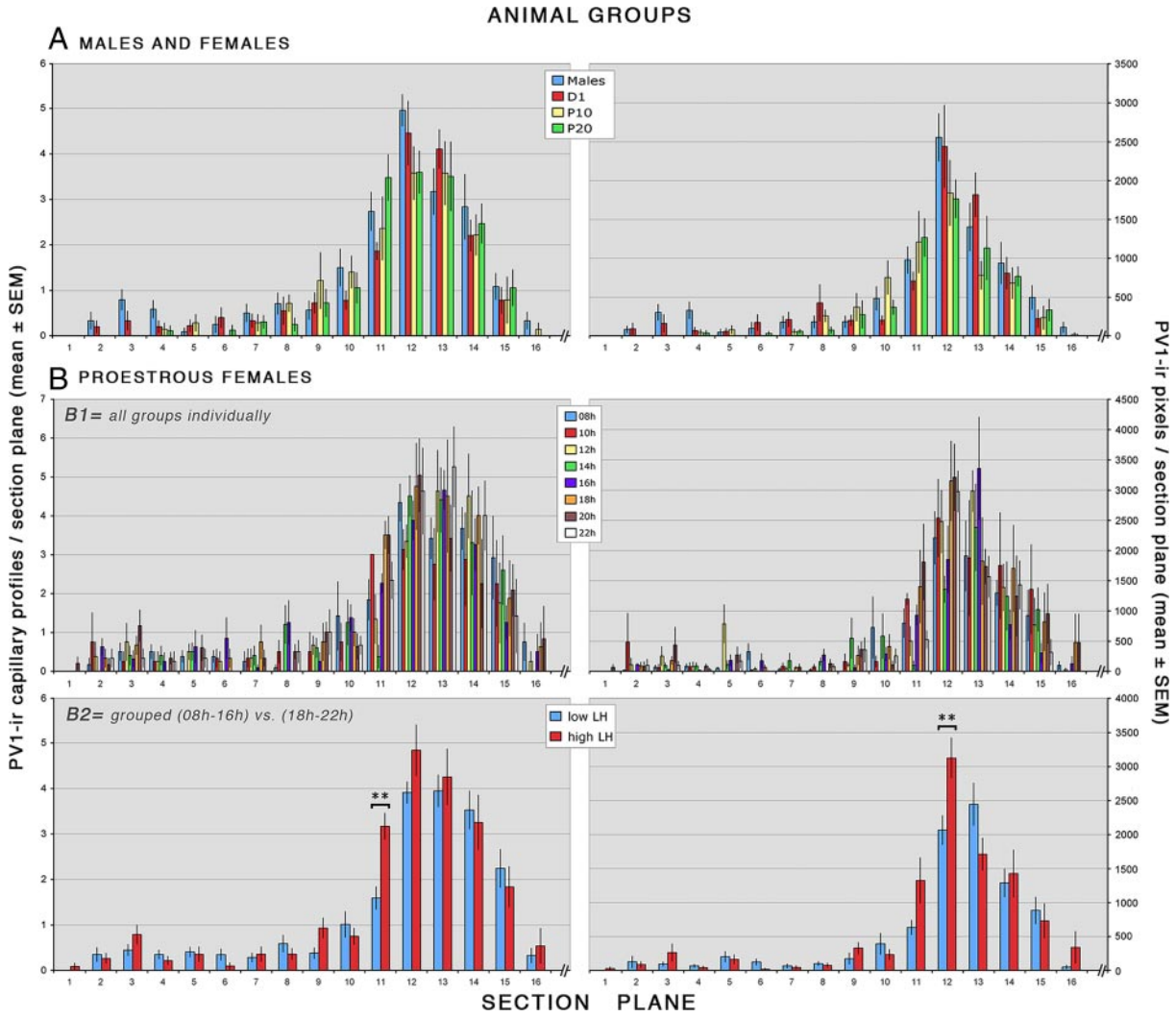

FIG. 6. Analysis of the distribution of PV1-labeling in the vmARC from section planes 1-16 in adult male and female rats (data are given as mean ± SEM numbers of PV1-ir capillary profiles and PV-ir pixels counted bilaterally; see *Materials and Methods*, supplemental Methods and supplemental Table 1). A, Comparison of males (n = 12) with females killed at 1000 h the day of diestrus 1 (D1; n = 10), or the day of proestrus at 1000 h (P10; n = 7) or 2000 h (P20; n = 9). B, Height groups of proestrous females killed every 2 h from 0800–2200 h (n = 4–6/time point). Statistical analysis was performed with groups either taken individually (B1) or grouped (B2) according to animals' low presurge (n = 23) or high surge (n = 14) LH levels (see supplemental Table 1). The two-way repeated measure ANOVA detected an effect of topography for all group comparisons, but no effect of sex/cycle (A) or time of the day (B1). In B2, there was, in addition by *post hoc* Tukey's multiple comparison test, an interaction (topography × LH) visible at planes 11 and 12 (**, $P < .01$). In A, B1, and B2, most section planes significantly differed from one another, which is not indicated for purpose of clarity.

by changes other than the expression of PV1 mRNA or protein. The observation that PV1 can display various glycosylation states indicates that hitherto undefined post-translational mechanisms may contribute to or dominate in dynamically modulating bidirectional blood-hypothalamus cross talk.

In the same vein, a striking sex difference in PV1 labeling may have been expected, due to the overt sex dimorphism in NKB labeling of perivascular axons seen in the vmARC/ME unit (16). In contrast, the present study failed to detect an overt male-to-female difference in distribution of PV1-positive microvessels in the vmARC. This is not paradoxical because our recent study (27) also failed to detect a sex dimorphism in vascular density in the vmARC. Moreover, our ultrastructural analyses of the vmARC (16) allowed us to clearly observe that perivascular axons do not directly touch capillary vessels but instead touch the barrier of ependymoglial tanycytes that constitute the real physical barrier between the blood and the parenchyma of the vmARC (15). Thus, the sex dimorphism in axonal phenotype may not resolve to a sex dimorphism in endothelial phenotype but may be linked to specific aspects of the dynamic control of the barrier of tanycytes and surrounding sensor neurons (as previously discussed in Refs. 16 and 27).

Labeling for PV1 was observed over every component of the hypothalamo-hypophysial vasculature including the SEP. The relevant question for peripheral feedback

integration involves the direction of blood flow in these microvessels. The evidence for rapid blood transport in the SEP to the vmARC is 2-fold: 1) a capillary permeability tracer injected in periphery entered the vmARC within seconds in the rat (14), and 2) by direct observation, after intracarotid dye injection, an upward flow of blood was indeed seen passing from the ME to the SEP of the vmARC in the dog (11). Additionally, it was shown in mice that iv injected horseradish peroxidase rapidly accumulates in the vmARC/ME (12) and it was demonstrated in rats that systemic administration of the ghrelin mimetic GHRP-6 activates vmARC neurons (37). Also, there is an attenuated expression of BBB-markers in the vmARC/ME unit (38, 39). Our observations of labeling for PV1 over the SEP now makes it likely that this is the specific conduit for fast peripheral feedback to arcuate sensor neurons. This conclusion fits with the congruent observations that the SEP forms postnatally (40), just before the arcuatotrophic surge of circulating leptin (41). Furthermore, because the vasculature of the vmARC/ME unit is anastomosed and permeable (Fig. 5 and supplemental Fig. 3; and Ref. 10), the SEP may also deliver to the vmARC substances released at the ME, *i.e.* the ultra-short loop feedback of neuroendocrine output.

The PV1-ir SEP capillaries are more abundant proximal to the pituitary stalk, *e.g.* to the gland itself. This topography supports the historic and debated issue of an upward, retrograde flow of blood from the gland to the vmARC for short loop feedback by pituitary hormones (10, 11, 17, 42). This hypothesis stemmed from the paradoxical observation in the rat that pituitary hormones are more concentrated in long portal vessels (upstream from the gland) than in peripheral circulation (downstream) (43). An upward flow of blood has been directly observed in the dorsal vasculature of the pituitary stalk after intracarotid dye injection in the pig (44). Magnetic resonance imaging in humans also detected an upward sequence of perfusion of the pituitary stalk (45, 46). However, in neither pigs nor humans was the blood flow seen to enter the ARC. This may have been due to methodological limitations and deserves further scrutiny. Obviously, when compared with other CVOs, the anatomophysiological specificity of the vmARC/ME unit is its proximity to the pituitary gland. In general, though, actions of peripheral hormones at the hypothalamus are rarely examined in the face of a modulatory role of pituitary hormones (47), and the integrated minute-by-minute pituitary activity during, for instance, an episode of food intake, remains insufficiently described.

Thus, blood flow to the vmARC through a permeable SEP may simultaneously convey neurohormonal ultrashort, pituitary short, and peripheral long feedback, *i.e.* allow acute adaptation of the balance between the hypothalamo-hypophysial gain and the hypophysio-peripheral gain (Fig. 7). This does not exclude other forms of chronic adaptation through less rapid or saturable avenues such as a paravascular flow of cerebrospinal fluid from the ME or classic transcytosis through the BBB-forming elements of the ARC (12, 14, 15, 48, 49). For example, the adipocyte hormone leptin may use several routes to act at different cell types and cellular levels through a variety of mechanisms (50–52). These routes notwithstanding, the presence of endothelial fenestrations in the microvasculature of the SEP may be a morphological argument for conceptually distinguishing fast/acute *vs.* slow/chronic feedback by a given lipid-insoluble signal. By analogy, lipophilic steroid hormones are now known to have such a dual feedback at cellular and/or neural-network levels by rapid (membrane effects) and delayed (genomic effects) mechanisms whose cross talk and respective contributions to hypothalamic activity are under intense investigation (see below). If so, whether arcuate neurons mediating acute and chronic feedback are different cells located close to or at a distance from fenestrated SEP capillaries, respectively, and corollary, how deep into the ARC an endogenous

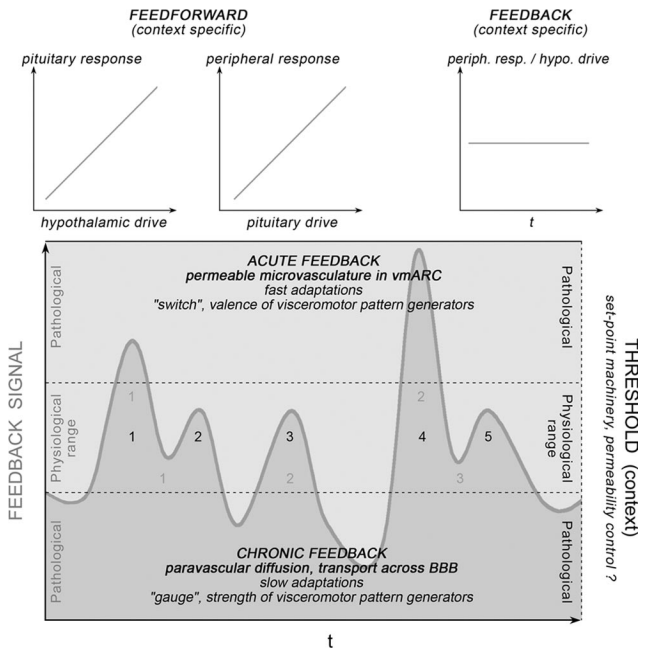

FIG. 7. Hypothesis of a biphasic action of circulating hormones upon the arcuate nucleus. *Top*, The role of the feedback sensor systems of the ARC is to ensure reliability of hypothalamic (hypo.) output in the face of peripheral (periph. resp.) sensitivity to pituitary action, *i.e.* in a context-specific manner. t, Time. *Bottom*, The sensor systems of the vmARC may be subjected to physiological regulation of their sensitivity (threshold) to both amplitude and frequency of feedback signal, *e.g.* as exemplified here, may be able to either see two, three, or five feedback pulses (*numbers in same row* indicate how many pulses would be detected at three different levels of sensitivity). See *Discussion*.

polypeptide can diffuse, are all critical and unanswered questions.

The ARC projects widely throughout the brain and influences directly or indirectly neural networks that are visceromotor pattern generators (VPGs) controlling metabolism and reproduction (53, 54). Tentatively (Fig. 7), an acute feedback at the vmARC may be a large-scale event that changes the valence of the output of VPGs, just like how rising plasma estradiol does in the morning of proestrus when it rapidly switches from a negative to a positive feedback action to trigger the preovulatory surge of LH (55) or how a corticosterone wave has a biphasic activating, then deactivating function (56). Conversely, a chronic feedback may dictate the strength of the output of VPGs by remaining below a given threshold. The rich, heterogeneous, and sexually dimorphic innervation of the vmARC region touching both ependymoglial tanycytes and neurons (16) is an indication that the threshold setpoint machinery is highly complex. Deregulation of this machinery may accompany metabolic disorders, and more generally, the current findings add a new locus at which altered function may produce neuroendocrine pathophysiologies.

Acknowledgments

We thank Dr. Francis Chaouloff for his expertise with statistics, Christel Poujol and Philippe Legros [both of the Plateforme d' Imagerie Cellulaire de l'Institut des Neurosciences, Institut Fédératif de Recherche no. 8 (IFR8), Université de Bordeaux2, Bordeaux, France] and the Electron Microscopy Facility of IFR14 (Institut de Médecine Prédictive, University de Lille 2, Lille, France).

This paper is dedicated to Professor Gérard Tramu in honor of his retirement.

Address all correspondence and requests for reprints to: Philippe Ciofi, Institut National de la Santé et de la Recherche Médicale Unité 862, Neurocentre Magendie, 146 rue Léo Saignat, F-33077 Bordeaux Cedex, France. E-mail: philippe.ciofi@inserm.fr.

This work was supported by Institut National de la Santé et de la Recherche Médicale, Centre National de la Recherche Scientifique, Université de Bordeaux, Université de Lille 2, La Fondation pour la Recherche Médicale and National Institutes of Health Grant P01 HD21921 to J.E.L.

Disclosure Summary: The authors have nothing to disclose.

References

1. **Grove KL, Grayson BE, Glavas MM, Xiao XQ, Smith MS** 2005 Development of metabolic systems. Physiol Behav 86:646–660
2. **Cone RD** 2006 Studies on the physiological functions of the melanocortin system. Endocr Rev 27:736–749
3. **Morton GJ, Cummings DE, Baskin DG, Barsh GS, Schwartz MW** 2006 Central nervous system control of food intake and body weight. Nature 443:289–295
4. **Plum L, Belgardt BF, Brüning JC** 2006 Central insulin action in energy and glucose homeostasis. J Clin Invest 116:1761–1766
5. **Badman MK, Flier JS** 2007 The adipocyte as an active participant in energy balance and metabolism. Gastroenterology 132:2103–2115
6. **Coll AP, Farooqi IS, O'Rahilly S** 2007 The hormonal control of food intake. Cell 129:251–262
7. **Gao Q, Horvath TL** 2007 Neurobiology of feeding and energy expenditure. Annu Rev Neurosci 30:367–398
8. **Williams KW, Scott MM, Elmquist JK** 2009 From observation to experimentation: leptin action in the mediobasal hypothalamus. Am J Clin Nutr 89:985S–990S
9. **Duvernoy H** 1972 The vascular architecture of the median eminence. In: Knigge KM, Scott DE, Weindl A, eds. Brain-endocrine interaction. Median eminence: structure and function. International Symposium Munich 1971. Basel: Karger; 79–108
10. **Ambach G, Palkovits M, Szentágothai J** 1976 Blood supply of the rat hypothalamus. IV. Retrochiasmatic area, median eminence, arcuate nucleus. Acta Morphol Acad Sci Hung 24:93–119
11. **Flerkó B** 1980 Fourth Geoffrey Harris Memorial Lecture: The hypophysial portal circulation today. Neuroendocrinology 30:56–63
12. **Broadwell RD, Balin BJ, Salcman M, Kaplan RS** 1983 Brain-blood barrier? Yes and no. Proc Natl Acad Sci USA 80:7352–7356
13. **Page RB** 1988 The anatomy of the hypothalamo-hypophysial complex. In: Knobil E, Neill J, Ewing LL, Greenwald GS, Markert CL, Pfaff DW, eds. The Physiology of Reproduction. 1st ed. New York: Raven Press; 1161–1233
14. **Shaver SW, Pang JJ, Wainman DS, Wall KM, Gross PM** 1992 Morphology and function of capillary networks in subregions of the rat tuber cinereum. Cell Tissue Res 267:437–448
15. **Rodríguez EM, Blázquez JL, Pastor FE, Peláez B, Peña P, Peruzzo B, Amat P** 2005 Hypothalamic tanycytes: a key component of brain-endocrine interaction. Int Rev Cytol 247:89–164
16. **Ciofi P, Leroy D, Tramu G** 2006 Sexual dimorphism in the organization of the rat hypothalamic infundibular area. Neuroscience 141:1731–1745
17. **Palkovits M** 2008 Stress-induced activation of neurons in the ventromedial arcuate nucleus: a blood-brain-CSF interface of the hypothalamus. Ann NY Acad Sci 1148:57–63
18. **Begley DJ, Brightman MW** 2003 Structural and functional aspects of the blood-brain barrier. Prog Drug Res 61:39–78
19. **Bearer EL, Orci L** 1985 Endothelial fenestral diaphragms: a quick-freeze, deep-etch study. J Cell Biol 100:418–428
20. **Stan RV** 2007 Endothelial stomatal and fenestral diaphragms in normal vessels and angiogenesis. J Cell Mol Med 11:621–643
21. **Stan RV, Kubitza M, Palade GE** 1999 PV-1 is a component of the fenestral and stomatal diaphragms in fenestrated endothelia. Proc Natl Acad Sci USA 96:13203–13207
22. **Goodman RL, Lehman MN, Smith JT, Coolen LM, de Oliveira CV, Jafarzadehshirazi MR, Pereira A, Iqbal J, Caraty A, Ciofi P, Clarke IJ** 2007 Kisspeptin neurons in the arcuate nucleus of the ewe express both dynorphin A and neurokinin B. Endocrinology 148:5752–5760
23. **Altarejos JY, Goebel N, Conkright MD, Inoue H, Xie J, Arias CM, Sawchenko PE, Montminy M** 2008 The Creb1 coactivator Crtc1 is required for energy balance and fertility. Nat Med 14:1112–1117
24. **Hill JW, Elmquist JK, Elias CF** 2008 Hypothalamic pathways linking energy balance and reproduction. Am J Physiol Endocrinol Metab 294:E827–E832
25. **Topaloglu AK, Reimann F, Guclu M, Yalin AS, Kotan LD, Porter KM, Serin A, Mungan NO, Cook JR, Ozbek MN, Imamoglu S, Akalin NS, Yuksel B, O'Rahilly S, Semple RK** 2009 TAC3 and TACR3 mutations in familial hypogonadotropic hypogonadism reveal a key role for Neurokinin B in the central control of reproduction. Nat Genet 41:354–358
26. **Ciofi P, Roca-Lapirot O, Garret M,** Immunocytochemical demonstration of fenestrated vessels in the rat hypothalamic arcuate nu-

cleus: a route for peripheral signals? Proc 36th Annual Meeting of the Society for Neuroscience, Washington, DC, 2005 (Abstract P242.1.2005)
27. **Ciofi P, Lapirot OC, Tramu G** 2007 An androgen-dependent sexual dimorphism visible at puberty in the rat hypothalamus. Neuroscience 146:630–642
28. **Stan RV, Ghitescu L, Jacobson BS, Palade GE** 1999 Isolation, cloning, and localization of rat PV-1, a novel endothelial caveolar protein. J Cell Biol 145:1189–1198
29. **Moragues N, Ciofi P, Lafon P, Odessa MF, Tramu G, Garret M** 2000 cDNA cloning and expression of a γ-aminobutyric acid A receptor ϵ-subunit in rat brain. Eur J Neurosci 12:4318–4330
30. **Moragues N, Ciofi P, Tramu G, Garret M** 2002 Localisation of GABA(A) receptor ϵ-subunit in cholinergic and aminergic neurones and evidence for co-distribution with the θ-subunit in rat brain. Neuroscience 111:657–669
31. **Ciofi P** 2000 Phenotypical segregation among female rat hypothalamic gonadotropin-releasing hormone neurons as revealed by the sexually dimorphic coexpression of cholecystokinin and neurotensin. Neuroscience 99:133–147
32. **Ciofi P, Krause JE, Prins GS, Mazzuca M** 1994 Presence of nuclear androgen receptor-like immunoreactivity in neurokinin B-containing neurons of the hypothalamic arcuate nucleus of the adult male rat. Neurosci Lett 182:193–196
33. **Paxinos G, Watson C** 1986 The rat brain in stereotaxic coordinates. 2nd ed. San Diego: Academic Press
34. **Carson-Walter EB, Hampton J, Shue E, Geynisman DM, Pillai PK, Sathanoori R, Madden SL, Hamilton RL, Walter KA** 2005 Plasmalemmal vesicle-associated protein-1 is a novel marker implicated in brain tumor angiogenesis. Clin Cancer Res 11:7643–7650
35. **Shue EH, Carson-Walter EB, Liu Y, Winans BN, Ali ZS, Chen J, Walter KA** 2008 Plasmalemmal vesicle-associated protein-1 (PV-1) is a marker of blood-brain barrier disruption in rodent models. BMC Neurosci 9:29
36. **Ballermann BJ, Stan RV** 2007 Resolved: capillary endothelium is a major contributor to the glomerular filtration barrier. J Am Soc Nephrol 18:2432–2438
37. **Dickson SL, Leng G, Robinson IC** 1993 Systemic administration of growth hormone-releasing peptide activates hypothalamic arcuate neurons. Neuroscience 53:303–306
38. **Rosenstein JM, Krum JM, Sternberger LA, Pulley MT, Sternberger NH** 1992 Immunocytochemical expression of the endothelial barrier antigen (EBA) during brain angiogenesis. Brain Res Dev Brain Res 66:47–54
39. **Norsted E, Gömüç B, Meister B** 2008 Protein components of the blood-brain barrier (BBB) in the mediobasal hypothalamus. J Chem Neuroanat 36:107–121
40. **Monroe BG, Paull WK** 1974 Ultrastructural changes in the hypothalamus during development and hypothalamic activity: the median eminence. Prog Brain Res 41:185–208
41. **Bouret SG, Gorski JN, Patterson CM, Chen S, Levin BE, Simerly RB** 2008 Hypothalamic neural projections are permanently disrupted in diet-induced obese rats. Cell Metab 7:179–185
42. **Page RB** 1982 Pituitary blood flow. Am J Physiol 243:E427–E442
43. **Oliver C, Mical RS, Porter JC** 1977 Hypothalamic-pituitary vasculature: evidence for retrograde blood flow in the pituitary stalk. Endocrinology 101:598–604
44. **Page RB** 1983 Directional pituitary blood flow: a microcinephotographic study. Endocrinology 112:157–165
45. **Sakamoto Y, Takahashi M, Korogi Y, Bussaka H, Ushio Y** 1991 Normal and abnormal pituitary glands: gadopentetate dimeglumine-enhanced MR imaging. Radiology 178:441–445
46. **Tien RD** 1992 Sequence of enhancement of various portions of the pituitary gland on gadolinium-enhanced MR images: correlation with regional blood supply. AJR Am J Roentgenol 158:651–654
47. **Sawchenko PE, Arias C** 1995 Evidence for short-loop feedback effects of ACTH on CRF and vasopressin expression in parvocellular neurosecretory neurons. J Neuroendocrinol 7:721–731
48. **Abbott NJ** 2004 Evidence for bulk flow of brain interstitial fluid: significance for physiology and pathology. Neurochem Int 45: 545–552
49. **Banks WA** 2009 Characteristics of compounds that cross the blood-brain barrier. BMC Neurol 9(Suppl 1):S3
50. **Münzberg H** 2008 Differential leptin access into the brain- A hierarchical organization of hypothalamic leptin target sites? Physiol Behav 94:664–669
51. **Pan W, Hsuchou H, He Y, Sakharkar A, Cain C, Yu C, Kastin AJ** 2008 Astrocyte leptin receptor (ObR) and leptin transport in adult-onset obese mice. Endocrinology 149:2798–2806
52. **Myers Jr MG, Münzberg H, Leinninger GM, Leschan RL** 2009 The geometry of leptin action in the brain: more complicated than a simple ARC. Cell Metab 9:117–123
53. **Thompson RH, Swanson LW** 2003 Structural characterization of a hypothalamic visceromotor pattern generator network. Brain Res Rev 41:153–202
54. **Simerly RB** 2005 Wired on hormones: endocrine regulation of hypothalamic development. Curr Opin Neurobiol 15:81–85
55. **McDevitt MA, Glidewell-Kenney C, Jimenez MA, Ahearn PC, Weiss J, Jameson JL, Levine JE** 2008 New insights into the classical and non-classical actions of estrogen: evidence from estrogen receptor knock-out and knock-in mice. Mol Cell Endocrinol 290:24–30
56. **de Kloet ER, Sarabdjitsingh RA** 2008 Everything has rhythm: focus on glucocorticoid pulsatility. Endocrinology 149:3241–3243